Photochemistry of Tertiary Nitrosoalkanes in Solid Polymer Matrices: A Promising New Class of Organic Materials for Holographic Recording with Semiconductor Lasers

J. Pinsl, M. Gehrtz,† A. Reggel, and Chr. Bräuchle*

Contribution of the Institut für Physikalische Chemie der Universität München, D-8000 München 2, FRG. *Received August 14, 1986*

Abstract: We have investigated a new class of photopolymers for near-infrared (near-IR) holographic recording: three members of the tertiary nitrosoalkanes (RNO) dissolved in two different poly(alkyl α-cyanoacrylates) (p-(alkyl-CAc)). Absorption/transmission spectroscopy, a CW holographic technique (PIH), and a newly developed phase-sensitive holographic technique, phase-modulated holography (PMH), were employed in these investigations. The last technique is an ideal tool for the investigation of photopolymer systems because it allows one to monitor separately and simultaneously the amplitude and phase contributions to the holographic grating and thus to monitor simultaneously the photoreaction of the RNO and the resulting holographic recording mechanism. The RNO in p-(alkyl-CAc) undergo a homolytic dissociation after absorption of one photon at wavelengths up to 799 nm. The corresponding photochemical rates, the quantum yields, and the activation energies were determined and were found to depend strongly on the glass transition temperature of the polymer solvent. However, hologram formation arises not only from the photoreaction of the RNO but mainly from a photoinduced expansion of the polymer matrix, i.e., a photomechanical effect. The resulting density change, which is associated with a large change of refractive index, does not depend on the RNO but on the matrix only. The near-IR holographic sensitivities of the new photopolymers were determined. They are high due to the considerable photomechanical effect, allowing one to write holographic gratings with a GaAlAs semiconductor laser at 788 nm.

1. Introduction

Near-infrared (near-IR) photoreactive compounds, when soluble in polymer matrices, are of great interest for developing near-IR-sensitive photopolymer systems employed, e.g., in integrated optics,[1,2] in holographic optical elements (HOES),[1] and as materials for holographic recording.[1-6] In all these applications low-cost semiconductor lasers, i.e., GaAlAs lasers emitting in the near-IR (750–900 nm), will be used preferentially as light sources for recording and reading.

In the case of holographic recording there are four other important demands for efficient recording materials besides the spectral sensitivity in the near-IR. The materials should show a high photosensitivity, a high resolution, high diffraction efficiencies, and the possibility of nondestructive reading.[1,5] There are no satisfactory recording materials in the near-IR wavelength region.[1,5-8] Photopolymer systems known to date additionally lack the high photosensitivity required, which is a major drawback for competing with conventional holographic recording materials based on silver halide emulsion, dichromated gelatin, or thermoplastics.[5] Thus, for applications with semiconductor lasers a photopolymer system with high photosensitivity in the near-IR has to be developed that also satisfies the other demands mentioned above.

C-Nitroso compounds are one of the very few classes of compounds that show an absorption maximum in the wavelength region from 600 to 790 nm,[9,10] i.e., up to the near-IR. The nitrosoalkanes in particular are found to undergo photolysis when illuminated with red light.[9-21] In order to investigate the suitability of nitrosoalkanes for holographic recording, it is necessary to investigate their photochemistry in solid polymer matrices, which may be different from the photochemistry of these compounds in liquid solution,[9-17] in the gas phase,[18,19] and in low-temperature rare-gas matrices[20,21] known from earlier studies. Further, for optimum performance of the near-IR-sensitive photopolymer systems in the applications mentioned above, the holographic recording mechanism has to be studied, too. We investigated the photochemical reaction and the holographic recording mechanism of three tertiary nitrosoalkanes dissolved in two different poly(alkyl α-cyanoacrylate) matrices. Transmission spectroscopy and CW holography,[3-6] both of which give characteristic parameters of the photoreaction,[3-5,22-25] as well as a newly developed phase-sensitive holographic technique[26,27] that provides unique information on

* To whom correspondence should be addressed.
† Present address: IBM Germany, D-6500 Mainz, FRG.

(1) Tomlinson, W. J.; Chandross, E. A. *Adv. Photochem.* **1980**, *12*, 201–281.
(2) Franke, H.; Festl, H. G.; Krätzig, E. *Colloid Polym. Sci.* **1984**, *262*, 213–216.
(3) Bräuchle, Chr.; Burland, D. M. *Angew. Chem., Int. Ed. Engl.* **1983**, *22*, 582–598.
(4) Bräuchle, Chr. *J. Mol. Cryst. Liq. Cryst.* **1983**, *96*, 83–98.
(5) Harihan, P. *Optical Holography*; Cambridge University Press: London, 1984; pp 88–115.
(6) Pinsl, J.; Deeg, F. W.; Bräuchle, Chr. *Appl. Phys. B* **1986**, *40*, 77–84.
(7) Gerbig, V.; Grygier, R. K.; Burland, D. M.; Sincerbox, G. *Opt. Lett.* **1983**, *8*, 404–406.
(8) Tatsuno, K.; Arimoto, A. *Appl. Opt.* **1980**, *19*, 2096–2102.
(9) Patai, S., Ed. *The Chemistry of Amino, Nitroso, and Nitro Compounds and Their Derivatives*; Wiley: Chichester, 1982; pp 181–290.
(10) Feuer, H., Ed. *The Chemistry of Nitro and Nitroso Groups*; Wiley: New York, 1969; Part 1, pp 137–213.
(11) Forrest, D.; Gowenlock, B. G.; Pfab, J. *J. Chem. Soc., Perkin Trans. 2* **1978**, 576–580.
(12) Forrest, D.; Gowenlock, B. G.; Pfab, J. *J. Chem. Soc., Perkin Trans. 2* **1977**, 12–15.
(13) Carmichael, P. J.; Gowenlock, B. G.; Johnson, C. A. F. *J. Chem. Soc., Perkin Trans. 2* **1973**, 1853–1856.
(14) v. Keussler, V.; Lüttke, W. *Z. Elektrochem.* **1959**, *63*, 614–623.
(15) Hammick, D. L.; Lister, M. W. *J. Chem. Soc.* **1937**, *489*–493.
(16) Anderson, K. D.; Crumpler, C. J.; Hammick, D. L. *J. Chem. Soc.* **1935**, 1679–1684.
(17) Mitchell, S.; Schwarzenwald, K.; Simpson, G. K. *J. Chem. Soc.* **1941**, 602–605.
(18) Keary, C. M.; Gowenlock, B. G.; Pfab, J. *J. Chem. Soc., Perkin Trans. 2* **1977**, 242–246.
(19) Mason, J. *J. Chem. Soc.* **1957**, 3904–3912.
(20) Müller, R. P.; Shigeo, M.; Nonella, M.; Huber, J. R. *Helv. Chim. Acta* **1984**, *67*, 953–958.
(21) Müller, R. P.; Huber, J. R. *Rev. Chem. Intermed.* **1984**, *5*, 423–457.
(22) Deeg, F. W.; Pinsl, J.; Bräuchle, Chr.; Voitländer, J. *J. Chem. Phys.* **1983**, *79*, 1229–1234.
(23) Bjorklund, G. C.; Burland, D. M.; Alvarez, D. C. *J. Chem. Phys.* **1980**, *73*, 4321–4328.
(24) Bräuchle, Chr.; Burland, D. M.; Bjorklund, G. C. *J. Am. Chem. Soc.* **1981**, *103*, 2515–2519.
(25) Deeg, F. W.; Pinsl, J.; Bräuchle, Chr. *J. Phys. Chem.* **1986**, *90*, 5715–5722.
(26) Pinsl, J.; Gehrtz, M.; Bräuchle, Chr. *J. Phys. Chem.* **1986**, *90*, 6754–6757.
(27) Gehrtz, M.; Pinsl, J.; Bräuchle, Chr. *Appl. Phys. B* **1987**, *43*, 61–77.

0002-7863/87/1509-6479$01.50/0

the holographic recording mechanism in the photopolymer system and simultaneously on the photochemistry of the photoreactive compound in the photopolymer system, were employed in these investigations.

Two of the nitroso compounds investigated undergo photolysis at illumination up to 799 nm. The number of photons involved in the photochemical mechanism, the photochemical rates, the quantum yields, and the activation energies are determined. Concerning the holographic recording mechanism, it was found that the primary photoprocess of the nitrosoalkane induces a transformation of the polymer matrix, which is accompanied by a photomechanical effect, i.e., an expansion of the polymer. This density change is responsible for the high holographic sensitivity of these new materials, which so far has not been equaled by other near-IR-sensitive organic holographic recording materials.[6,7] It was indeed possible to write holograms with a GaAlAs laser at 788.1 nm in these photopolymers. Holographic sensitivities were determined for the near-IR region up to 799 nm.

2. Phase-Insensitive CW Holography and Phase-Modulated Holography: Theoretical Background and Comparison

2.1. Phase-Insensitive CW Holography (PIH). The interference of two coherent laser beams superimposed on a photoreactive sample results in a sinusoidal intensity distribution of the laser light. The photochemistry taking place transforms this intensity distribution into a corresponding distribution of photoproducts and educts. A sinusoidal modulation of the absorption coefficient a and the index of refraction n is produced,[3-7,22-26] i.e., an amplitude grating and a phase grating yielding together the complete holographic grating. The growth of the modulation amplitudes of the absorption coefficient $a_1(t)$ and the index of refraction $n_1(t)$ includes the kinetics of the photochemical reaction. The kinetic parameters of such a reaction can be revealed by observing the time dependence of the diffraction efficiency $\eta(t)$ of the holographic grating. When the grating is illuminated with a laser beam at wavelength λ under the appropriate angle θ (the Bragg angle), the laser beam is diffracted with diffraction efficiency $\eta(t)$[27]

$$\eta(t) = I_{diff}/I_{det} = [P^2(t) + A^2(t)]D^2 \quad (1a)$$

where I_{diff} and I_{det} are the intensities of the diffracted beam and the detection beam and D is a loss factor due to the average optical density $\overline{OD}$ of the material at

$$D(\lambda) = \exp(-1.15\overline{OD}(\lambda)/\cos\theta) \quad (1b)$$

For small diffraction efficiencies, i.e., for early times in the holographic growth process, the diffraction amplitude of the phase grating P is given by

$$P(t) = (\pi d/2\cos\theta)n_1(t) \quad (2a)$$

and the diffraction amplitude of the amplitude grating A is given by

$$A(t) = (d/2\cos\theta)a_1(t) \quad (2b)$$

For a simple one-step photoreaction with an underlying one-photon, two-level mechanism, A and P are linear in time in the small reaction yield limit;[23] i.e.

$$P(t) = -2303c_0\epsilon_{rec}Q\Delta R_{eff}[\pi d/(\lambda\cos\theta)]I\phi t \quad (3a)$$

for the educt as the absorbing species at λ and

$$A(t) = 2303c_0\epsilon_{det}\epsilon_{rec}(2.303/4)(d/\cos\theta)I\phi t \quad (3b)$$

Accordingly, the holographic growth curves $\eta(t)$ are quadratic in time

$$\eta(t) = at^2 \quad (4a)$$

$$\eta^{1/2}(t) = a^{1/2}t \quad (4b)$$

with a "slope" $a^{1/2}$. In eq 3 ϵ_{rec} is the extinction coefficient of the recording wavelength, c_0 is the initial concentration of the educt, I is the recording intensity, ϕ is the quantum yield for the product formation, ΔR_{eff} is the change of molar refraction, and ϵ_{det} is the extinction coefficient at the detection wavelength λ. The factor Q, which arises from the Lorenz–Lorentz relation,[1,29] is given by

$$Q = (n^2 + 2)^2/6000n \quad (4c)$$

where n is the average refractive index of the material. From the slope $a^{1/2}$ the quantum yield ϕ can be determined provided one knows the change of molar refraction ΔR_{eff}.[22] On the other hand, $|\Delta R_{eff}|$ can be determined provided one knows ϕ. (The rest of the parameters in eq 3a are well-known from the arrangement of the holographic experiment and from absorption spectroscopy.) For a pure phase hologram, i.e., $\epsilon_{del} \to 0$, term two in eq 1a vanishes and the grating is based on changes of the refractive index only.

2.2. Changes of the Molar Refraction Induced by Photochemical Reactions. ΔR_{eff}, the change of molar refraction between product and educt of a photoreaction, is a quantity that is not easily accessible. It is responsible for the formation of the phase grating by a photochemical transformation. The absolute value of the change of molar refraction, $|\Delta R_{eff}|$, can be determined from holographic growth curves according to

$$|\Delta R_{eff}| = [(a^{1/2}/2303\epsilon_{rec}c_0dI\phi D)^2 - (2.303\epsilon_{det}/4\cos\theta)^2]^{1/2}(\lambda\cos\theta/\pi Q) \quad (5)$$

A wavelength-dependent measurement of the diffraction efficiency yields the wavelength dependence of $|\Delta R_{eff}|(\lambda)$. In order to measure this dependence it is favorable to define a normalized diffraction efficiency $\gamma(\lambda)$

$$\gamma(\lambda) = a^{1/2}(\lambda)/\epsilon_{rec}c_0dI$$

$$\gamma(\lambda) = 2303\phi\{[(\pi/\lambda\cos\theta)Q|\Delta R_{eff}|(\lambda)]^2 + (2.303\epsilon_{det}/4\cos\theta)^2\}^{1/2}D(\lambda) \quad (6)$$

A second possibility for obtaining the change of molar refraction ΔR_{PC} due to a photochemical transformation is to use the Kramers–Kronig formulas, which relate the molar refractions of product R_P and educt R_E to the absorption maxima of product and educt by[30]

$$\Delta R_{P,E}(\lambda) = (2303/3\pi^2cd)\int_s OD_s(\lambda)\,d\lambda/\{[1 - (\lambda_s/\lambda)]^2 + \gamma_s^2/\lambda[1 - (\lambda_s/\lambda)^2]\} \quad (7a)$$

$$\Delta R_{PC}(\lambda) = R_P(\lambda) - R_E(\lambda) \quad (7b)$$

In eq 7a, c is the velocity of light, OD_s is the optical density of the homogeneous broadened absorption maximum s with the central wavelength λ_s, and γ_s is the damping constant in units of wavelength. Equation 7 allows one to calculate $\Delta R_{PC}(\lambda)$, provided one knows the complete absorption spectra of product and educt. This is in general not the case for the far-UV region, but for most photoreactions leading to a rearrangement of valence electrons only, there are no big differences in the far-UV absorption between product and educt.

Comparison of the holographically determined $|\Delta R_{eff}|(\lambda)$ and $\Delta R_{PC}(\lambda)$ shows in some cases that the two values are *not* identical, but differ considerably by a value K that does *not* depend on the wavelength.

$$|\Delta R_{eff}|(\lambda) = |\Delta R_{PC}(\lambda) + K| \quad (8a)$$

For $K \neq 0$ the phase grating is produced not only by a photochemical transformation but also by a density change generated in the polymer matrix.[1,6,25]

$$K = (n^2 - 1)(10^3\Delta\rho/[(n^2 + 2)c_0\rho_P]) \quad (8b)$$

This change of the overall density induced by a photochemical transformation is called a photomechanical effect.[31] In eq 8b ρ_P is the density of the material after the photoreaction is complete, and $\Delta\rho$ is the corresponding density change. In eq 8a,b it has been assumed that the density change $\Delta\rho(t)$ is proportional to the

(28) Kogelnick, H. *Bell Syst. Tech. J.* **1969**, *48*, 2909–2947.
(29) Jackson, J. D. *Classical Electrodynamics*; Wiley: New York, 1962; pp 155–158.
(30) Deeg, F. W. Thesis, University of Munich, 1986.
(31) Smets, G. *Adv. Polym. Sci.* **1983**, *50*, 17–44.

concentration of the photoreactive component $c(t)$. $\Delta\rho$ can be positive, corresponding to a shrinkage of the polymer matrix, or negative, corresponding to an expansion. With PIH measurements the sign of ΔR_{eff} cannot be determined, and the sign and the exact value of K can only be inferred from wavelength-dependent detection of hologram growth outside the absorption bands where $\gamma(\lambda)$ is not determined by $D(\lambda)$ but by $\Delta R_{eff}(\lambda)$ (see eq 6). This was shown in detail in ref 6. However, employing the newly developed method of phase-modulated holography, it is much easier to obtain *directly* the sign and value of ΔR_{eff} and of K.[26,27]

2.3. Phase-Modulated Holography (PMH). With phase-insensitive holography (PIH) the overall diffraction efficiency η cannot be separated into its dispersive (P) and absorptive part (A), and the absolute signs of A and P and thus also the sign of ΔR_{eff} are lost (see eq 2a). A recently achieved advance in the holographic grating methods, using phase-modulation techniques (PMH), however, allows one to monitor the phase and amplitude gratings separately and simultaneously and to measure directly the values and the absolute signs of A and P.[26,27] ΔR_{eff}, including its sign, can then be determined from PMH according to[26,27]

$$\Delta R_{eff} = -(P/A)(0.58\epsilon_{det}\lambda_{det}/(\pi Q)) \quad (9)$$

Knowing the sign of ΔR_{eff} and the value of K, one can determine the corresponding $\Delta\rho$ from eq 8a and 8b.

The full theoretical framework for PMH is developed in detail in ref 27. Here we restrict ourselves to a brief overview. In PMH one of the two overlapping laser beams has its phase φ modulated with an electrooptic modulator (EOM)

$$\varphi(t) = M \sin(\omega_m t) \quad (10)$$

where M is the modulation index and ω_m is the modulation frequency. Accordingly the electric field amplitude E'_m of the modulated (m) beam after the sample (see Figure 2) is

$$E'_m = DE_m e^{i\varphi(t)} \quad (11)$$

Considering the other beam, i.e., the reference (r) beam, which is partly diffracted in the direction of the m-beam, the diffracted amplitude E_d is given by coupled wave theory[28] as

$$E_d = -D(iP + A)E_r \quad (12)$$

where E_r is the electric field amplitude of the r-beam. Note the $\pi/2$ phase difference between P and A (i.e., the i in eq 12), which will lead to the separation of P and A. Detection in the direction of the m-beam with a square-law photodetector results in the detection of a homodyne beat signal proportional to $S(t)$

$$S(t) = |E'_m + E_d|^2 \quad (13)$$

Two relevant signals[26,27] are produced, one at the fundamental of the modulation frequency ω_m, which is proportional to P

$$U_1(t) = -2D^2\Sigma(F_m F_r)^{1/2} MP(t) \sin(\omega_m t) \quad (14a)$$

and a second signal at $2\omega_m$ that is proportional to A

$$U_2(t) = -2D^2\Sigma(F_m F_r)^{1/2}(M^2/4)A(t) \cos(2\omega_m t) \quad (14b)$$

In eq 14a and 14b Σ is the overall detection sensitivity (in V/W) and $F_{m,r}$ are the integrated beam powers of the m- and r-beams (in W). According to eq 14a and 14b, P and A can be monitored separately and simultaneously at ω_m and $2\omega_m$ using two lock-in amplifiers. From the ratio (P/A), ΔR_{eff} can be readily determined (see eq 9).

Note further that the quantum yield ϕ of a photoreaction cannot be determined from PIH measurements if a photomechanical effect arises with $K \neq 0$, provided the sign and the value of K are not exactly known. However, with PMH it is possible to measure *simultaneously* the photomechanical effect via P (see eq 8 and 9) and the quantum yield ϕ via A (see eq 3b).

3. Experimental Section

3.1. Setup for Phase-Insensitive CW Holography (PIH). The PIH measurements were performed with the usual setup[3-7,22-25] (Figure 1). Recording was accomplished at wavelengths from 530.9 to 799.3 nm using a krypton laser (Coherent Innova 100 K3), a krypton pumped dye laser (Coherent CR 699-02), a GaAlAs laser (Hitachi HL 7801 E), and a He–Ne laser (NEC GLG 5700/S 5702). The laser beam was vertically polarized and split into two beams, the reference and object beams which were superimposed on the sample. The reference and object beams were focused, giving $1/e$ radii varying between 1 mm and 70 μm. Care was taken that both beams had the same power density to get a fringe contrast of unity. The growing hologram was monitored by means of the reference beam, using a double chopper that periodically (100 Hz) turned on and off the object beam. The fringe spacings recorded varied between 4.3 and 0.75 μm.

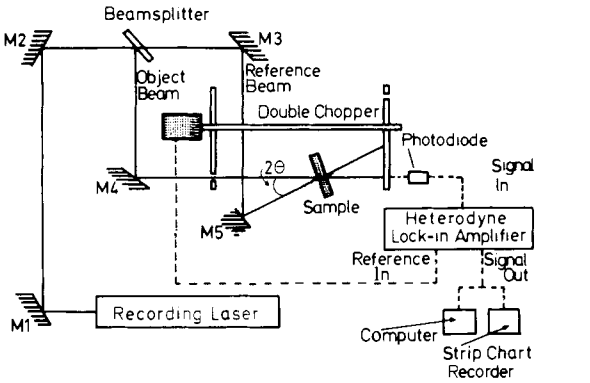

Figure 1. Experimental setup for phase-insensitive CW holography (PIH). M_1 to M_5 are mirrors.

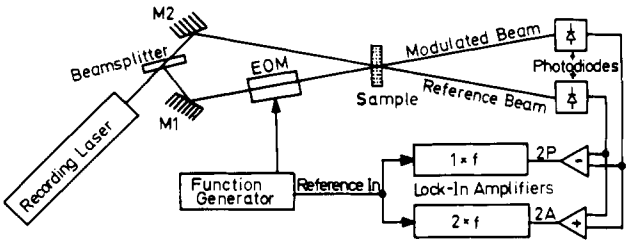

Figure 2. Experimental setup for phase-modulated holography (PMH) in the dual-beam version. M_1 and M_2 are mirrors, and EOM is the electrooptic modulator crystal.

3.2. Setup for Phase-Modulated Holography (PMH). The setup for the phase-modulated holographic experiment is described in detail in ref 26 and 27. The apparatus is schematically shown in Figure 2. A krypton laser with an intracavity etalon (coherence length >2.0 m) and a He–Ne laser (coherence length 0.05 m) were used for recording. The recording laser beam was split into two beams, the modulated (m) beam and the reference (r) beam. The m-beam was focused into an electrooptic modulator crystal (EOM) of $LiTaO_3$, recollimated after the crystal, and then superimposed with the r-beam at the sample. The m-beam's optical phase φ is modulated (see eq 10) by feeding the output of a function generator (Systron Donner 420) to the EOM. A modulation index of M = 0.7 was employed in most of the experiments, and the modulation frequency was $\omega_m/2\pi$ = 1.2 kHz.

Signal detection and processing were carried out in most of the experiments with the dual-beam PMH technique. Two matched photodiodes (Siemens SFH 202 silicon p–i–n) were placed in the direction of the m- and r-beams behind the sample. The photocurrents were added and subtracted, amplified, and high-pass filtered. The resulting signals U_1 and U_2 (see eq 14a and 14b) were monitored by two lock-in amplifiers, an Ithaco 391A at ω_m, i.e., in the $1 \times f$ mode, and an Ithaco 393A at the second harmonic of ω_m, i.e., in the $2 \times f$ mode.

3.3. Absorption/Transmission Spectroscopy. The absorption spectra were recorded with a spectrophotometer (Perkin-Elmer Model 330). In the low-temperature experiments an optical cryostat (Oxford CF 204) containing the sample was positioned in the spectrophotometer. With this apparatus the photoreactive sample could be illuminated with a laser beam at low temperature and subsequently the corresponding absorption spectrum could be recorded. The experiments were performed at various temperatures to determine the activation energy of the photoreaction.

For measuring the quantum yields the time dependence of the intensity of a chopped laser beam transmitted through the sample was monitored with the help of a photodiode (UDT PIN 10D/UV) and a lock-in amplifier (Ithaco 393A). This method was found to give more accurate results than absorption spectroscopy, where the progress of the reaction is monitored from decreasing or increasing absorption bands in the spectrum. Monitoring the transmission has the advantage that the sample is not moved during the experiment and that the illuminated and

Table I. Central Wavelength of the Absorption Maximum λ_0, Activation Energy E_A, and Quantum Yield of the Photodissociations ϕ_{TS} Determined from Transmission Spectroscopy and ϕ_{PMH} Determined from PMH Measurements for RNO/p-(Alkyl-CAc)[a]

	λ_0, nm	E_A, kcal/mol	ϕ_{TS}	ϕ_{PMH}	ϕ^{*a}
MNP/p-(EtCAc)	678	0.77	$(1.12 \pm 0.12) \times 10^{-2}$	$(1.03 \pm 0.26) \times 10^{-2}$	
TENC/p-(EtCAc)	688	0.70	$(7.00 \pm 2.30) \times 10^{-2}$	$(8.08 \pm 2.26) \times 10^{-2}$	1.94[b]
NCPA/p-(EtCAc)	648	0.83	$(8.91 \pm 3.52) \times 10^{-3}$	$(7.94 \pm 1.35) \times 10^{-3}$	1.05[c]
MNP/p-(MeCAc)	678	1.55	$(4.67 \pm 0.70) \times 10^{-3}$	$(5.30 \pm 1.13) \times 10^{-3}$	
TENC/p-(MeCAc)	688	1.42	$(2.64 \pm 0.32) \times 10^{-2}$	$(2.20 \pm 0.45) \times 10^{-2}$	
NCPA/p-(MeCAc)	648	1.38	$(2.83 \pm 0.78) \times 10^{-3}$	$(3.35 \pm 0.71) \times 10^{-3}$	

[a] ϕ^* is the quantum yield for the photodissociation of the RNO in liquid solution taken from the literature. [b] Quantum yield of the photolysis of TENC in methanol.[15] [c] Quantum yield of the photolysis of NCPA in methanol.[17]

observed spots on the sample are identical, which is necessary for exact calculations of the quantum yield. Note that the Gaussian beam profile has to be taken into account, leading to a signal $U(t)$

$$U(t) = U_0 + 1.15U_0OD_0(2303\epsilon_{rec}\phi ICt) \quad (15)$$

In eq 15 U_0 is the signal produced at the beginning of the reaction and OD_0 is the initial optical density of the sample at the detection wavelength.

3.4. Sample Preparation. The tertiary nitrosoalkanes (RNO) 2-methyl-2-nitrosopropane (MNP), 2-chloro-2,3-dimethyl-3-nitrosobutane (TENC), and 4-nitroso-4-chloropentanoic acid (NCPA) were dissolved in the monomers ethyl α-cyanoacrylate (m-(EtCAc)) and methyl α-cyanoacrylate (m-(MeCAc)), respectively. The concentrations ranged between 0.1 and 0.5 mol/L. The RNO-doped monomers were squeezed between two microscopic slides with spacers of various thickness and allowed to polymerize. After 36 h for m-(EtCAc) and 28 h for m-(MeCAc) at room temperature in the dark thin polymer films of good optical quality were obtained.

Pure m-(EtCAc) and m-(MeCAc) were purchased from Schering AG and used without further purification. MNP was supplied by Aldrich in its dimer form. TENC and NCPA were prepared by known methods.[17,32] MNP and TENC were used without further purification. NCPA was recrystallized from hexane (spectroscopic grade) before use. In general, the monomer crystalline nitroso compounds have a very high vapor pressure[32] and are easily oxidizable. Thus the compounds should be stored in a refrigerator in the dark under nitrogen and in a sealed flask. The doped polymer films should be kept between microscopic slides and the latter should be sealed with Teflon tape because Teflon is an effective barrier to oxygen and RNO vapor. Alkyl α-cyanoacrylates, which are often used as hosts in organic holographic material research,[6,7,33] form an excellent matrix for the RNO because of their fast polymerization at room temperature by radical or mainly anionic initiation,[34] thus confining the RNO in the polymer.

The nitrosoalkanes should be handled with caution, because aromatic *C*-nitroso compounds are suspected to be mutagenic and carcinogenic.[35]

4. Results and Discussion

4.1. Photochemistry of Tertiary Nitrosoalkanes in Solid Poly(alkyl α-cyanoacrylates). From liquid solution and gas-phase spectroscopy it is known[9,10] that *C*-nitroso compounds in their monomer form show a characteristic low-intensity absorption maximum around 700 nm ($\epsilon \sim 1$–20) due to a singlet–singlet transition of the lone electron pair on nitrogen, a further absorption maximum around 280 nm ($\epsilon \sim 100$) due to an $n-\pi^*$ transition of the oxygen lone electron pair, and a rather intense absorption band around 220 nm ($\epsilon \sim 5000$), which has been assigned to the $\pi-\pi^*$ transition of the NO group. Nitrosoalkanes are photochemically unstable when illuminated at the long-wavelength absorption maximum. Primary and secondary nitrosoalkanes tautomerize easily to oximes. This reaction is accelerated upon illumination.[10] Tertiary nitrosoalkanes are relatively stable; however, a light-induced homolysis of the C–N bond is observed, producing alkyl and nitric oxide radicals with a subsequent self-scavenging reaction in liquid solution[9–13] (see Figure 3).

We investigated the photochemistry of the three tertiary nitrosoalkanes (RNO) 2-methyl-2-nitrosopropane (MNP), 2-chloro-2,3-dimethyl-3-nitrosobutane (TENC), and 4-nitroso-4-chloropentanoic acid (NCPA) (see Figure 3) dissolved in solid poly(methyl α-cyanoacrylate) (p-(MeCAc)) and poly(ethyl α-cyanoacrylate) (p-(EtCAc)). All three RNO show the absorption maximum in the red (see Figure 4 and Table I) and they undergo photolysis when illuminated with visible or near-IR light at wavelengths up to 799.3 nm. After photolysis the sample is bleached; i.e., the long-wavelength absorption maximum vanishes and in the case of TENC and MNP the absorption band at 280 nm vanishes, too (see Figure 4). Nitrosobenzene dissolved in the polymers was also investigated and found to undergo photolysis only when illuminated with UV light. This result is in agreement with former results concerning the liquid solution photochemistry of aromatic *C*-nitroso compounds.[9,10]

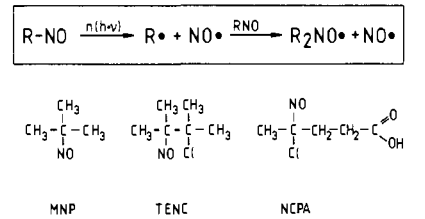

Figure 3. Basic photoprocess and subsequent self-scavenging reaction of tertiary nitrosoalkanes in liquid solution.[9-13]

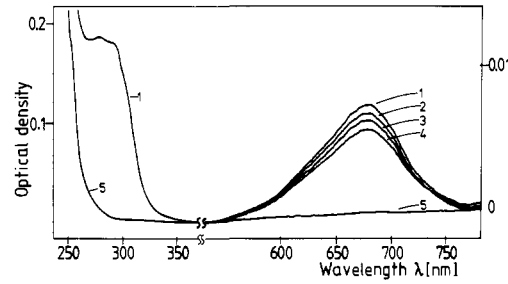

Figure 4. Absorption spectra of MNP/p-(EtCAc) ($c_0 = 0.5$ mol/L): (1) before illumination; (2–4) after successive illumination with laser light at $\lambda = 752.5$ nm and $I = 1.05$ W/cm^2; (5) after complete photoreaction.

Since many nitroso compounds are in equilibrium with their azodioxy dimers RN(O)N(O)R,[9,10,14] in the solid state and in solution the extinction coefficient of the long-wavelength absorption maximum often depends on concentration, temperature, and solvent. MNP is completely dimerized in the solid state.[11,16] TENC and NCPA, however, exist to a fairly large extent in the monomeric form,[17,32] as indicated by the dark blue color of the crystals. Upon dissolving in the polymer matrix in moderate concentrations all three RNO monomerize. This was confirmed by our concentration-dependent measurements of the extinction coefficients of the long-wavelength absorption band. The extinction coefficients were found to be independent of concentration for TENC and NCPA. For MNP only, at concentrations >0.8 mol/L increased dimerization was observed, leading to a strong maximum around 290 nm ($\epsilon \sim 4000$), which arises from a $\pi-\pi^*$ transition of the dinitroso group ONNO.[9,10,14]

4.1.1. Activation Energies and Quantum Yields. The absorption spectra of the RNO at 10 K show a narrowing of the near-IR absorption band, indicating inhomogeneous broadening of the transition at low temperature. However, photochemistry can only be observed above 100 K. At these higher temperatures the

(32) Thiele, J. *Ber.* **1894**, *27*, 454–457.
(33) Friesen, E.; Rav; Noy, Z.; Reich, S. *Appl. Opt.* **1977**, *16*, 427–432.
(34) Elias, H. G. *Makromoleküle*; Hüthig & Wepf: Basel, 1981; p 767–768.
(35) Mulder, G. J.; Kadlubar, F. F.; Mays, J. B.; Hinson, J. A. *Mol. Pharmacol.* **1984**, *26*, 342–347.

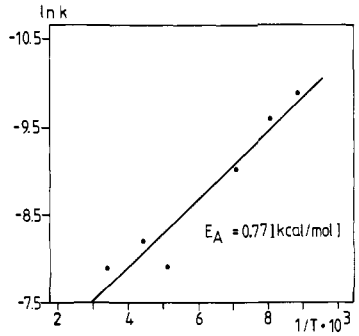

Figure 5. Arrhenius plot for the photoreaction of MNP/p-(EtCAc).

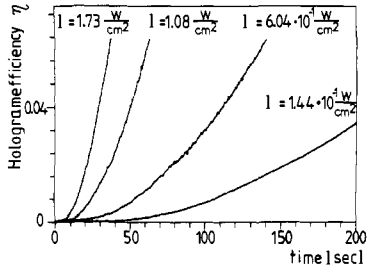

Figure 6. Four holographic growth curves in MNP/p-EtCAc at four different intensities (λ = 752.5 nm).

absorption band is homogeneously broadened; i.e., the photoreaction of RNO merely induces a decrease of the complete absorption band (see Figure 4). Neither photophysical nor photochemical holes[36] could be burnt in the near-IR absorption band of the RNO by illumination with laser light at wavelengths between 600 and 700 nm. From the decrease of the absorption maximum the photochemical rate was determined at various temperatures for all three RNO compounds dissolved in p-(EtCAc) and p-(MeCAc). The corresponding Arrhenius plot for MNP in p-(EtCAc) is depicted in Figure 5. The activation energies are collected in Table I. All three RNO show rather similar activation energies depending, however, strongly on the polymer matrix used. The higher activation energy is associated with the higher glass transition temperature of p-(MeCAc) (T_g = 177 °C) compared to p-(EtCAc), where T_g = 115 °C.[6] A higher glass transition temperature usually corresponds to a more rigid framework of the polymer matrix[34] at room temperature and can influence considerably the photoreactivity with the matrix via chain segment mobility.

The quantum yields for the three RNO in the solid polymer matrix were determined with the help of transmission spectroscopy (see eq 15) and from measurements of A with PMH according to eq 3b. The values are compared in Table I and show good agreement. They are relatively small compared to the quantum yields found for the photoreaction of the compounds in liquid solution. The liquid solution results depend on the solvent[12,15] and can exceed unity[12,15] because of the self-scavenging reaction following homolysis (see Figure 3). The low quantum yields in the solid polymer matrix probably arise from the limited mobility of the homolytically generated radicals, leading to a higher rate of recombination for the radicals in their solvent cage. According to the activation energies the quantum yields found in p-(EtCAc) are higher than in p-(MeCAc). This effect was already observed in previous investigations concerning the photoreaction of benzophenone[25] in various poly(alkyl acrylates), where the quantum yield depends strongly on T_g, too.

4.1.2. Photochemical Mechanism. The photochemical mechanisms of the RNO photoreaction were investigated by PIH by evaluating holographic growth curves recorded with varying excitation intensities. The experiments were performed at λ = 752.5 and 799.3 nm. In Figure 6 four holographic growth curves in MNP/p-EtCAc at λ = 752 nm at four different recording intensities I are shown. According to eq 4, the least-squares fit of a log–log plot of the slope of the curves, $a^{1/2}$, vs recording intensity should result in a straight line with a slope of unity for a one-photon mechanism.[3-5,22-25] For MNP in p-(EtCAc) at λ = 752.5 nm the graph is shown in Figure 7. It has indeed a slope of unity as do the corresponding graphs for TENC and NCPA.

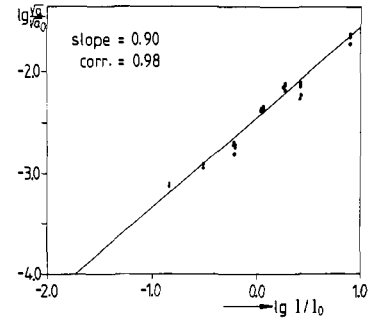

Figure 7. log–log plot of the "slope" of the holographic growth curves $a^{1/2}$ vs recording intensity I for MNP/p-(EtCAc) (λ = 752.5 nm, $a_0^{1/2}$ = 1 s^{-1}, I_0 = 1 W/cm²).

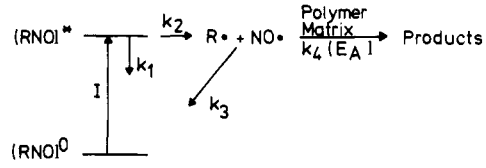

Figure 8. Reaction scheme for the photoreaction of RNO occurring in p-(alkyl-CAc). I = recording intensity, k_1 = photophysical relaxation rate, k_2 = photochemical rate, k_3 = recombination rate, and k_4 = rate of the subsequent reaction between radicals and polymer matrix.

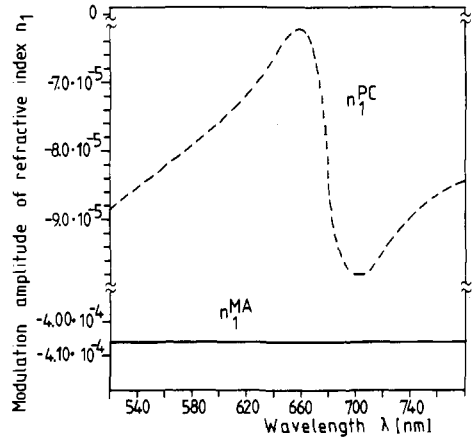

Figure 9. Modulation amplitude of the refractive index vs wavelength due to pure photochemistry (n_1^{PC}) (---) and due to the photomechanical effect (n_1^{MA}) (—) in a 10-day-old sample of MNP/p-(EtCAc) after complete photolysis.

In conclusion we propose the reaction scheme shown in Figure 8. After absorption of one photon in the near-IR, i.e., excitation of the first excited singlet state, the RNO homolytically dissociates to alkyl and nitric oxide radicals. From the small quantum yields and the T_g dependence of quantum yields and activation energies we conclude that cage recombination (k_3) and reaction with the polymer chains of the matrix (k_4) are competitive reaction pathways for the radical pair. The reaction of the radical pair with the matrix seems to be the activation energy controlled reaction step because the activation energy is similar for all three RNO but different for the two polymer matrices. This result largely excludes the possibility of an excited-state barrier. A reduced quantum yield due to radical recombination was found in solution photochemistry, too, together with a decrease of the quantum yield with increasing solvent viscosity.[15]

4.2. Holographic Recording Mechanism. From the absorption spectra of product and educt of the RNO/p-(alkyl-CAc) photo-

(36) Friedrich, J.; Haarer, D. *Angew. Chem., Int. Ed. Engl.* **1984**, *23*, 113–140.

Table II. Calculated Change of Molar Refraction (ΔR_{PC}), Ratio of Phase to Amplitude Hologram Efficiency (P/A), Change of Molar Refraction Measured by PMH (ΔR_{eff}), Change of Molar Refraction Measured by PIH ($|\Delta R_{eff}|$), and K[a]

	ΔR_{PC}, cm³/mol	P/A	ΔR_{eff}, cm³/mol	$\lvert\Delta R_{eff}\rvert$, cm³/mol	K, cm³/mol
MNP/p-(EtCAc)	−0.33	(5.71 ± 1.08) × 10^2	−26.38 ± 5.01	28.39 ± 6.53	−28.06 ± 6.45
TENC/p-(EtCAc)	−0.39	(9.52 ± 1.99) × 10^2	−46.20 ± 9.70	36.22 ± 5.43	−35.83 ± 5.37
NCPA/p-(EtCAc)	0.45	(4.20 ± 1.09) × 10^2	−27.50 ± 7.15	27.83 ± 7.19	−28.28 ± 7.31
MNP/p-(MeCAc)	−0.33	(2.41 ± 0.53) × 10^2	−11.13 ± 2.45	12.70 ± 2.29	−12.37 ± 2.23
TENC/p-(MeCAc)	−0.39	(3.06 ± 0.70) × 10^2	−14.85 ± 3.44	15.65 ± 2.19	−15.26 ± 2.14
NCPA/p-(MeCAc)	0.45	(1.86 ± 0.45) × 10^2	−12.15 ± 2.92	9.42 ± 2.26	−9.87 ± 2.37

[a] All values are calculated for and measured at λ = 632.8 nm.

Table III. K Values and Corresponding Relative Density Change $\Delta\rho/(\rho_P c_0)$ for MNP/p-(EtCAc) Samples of Two Different Ages Measured at Two Different Wavelengths λ

	λ = 632.8 nm		λ = 752.5 nm	
	K, cm³/mol	$\Delta\rho/(\rho_P c_0)$, 1/mol	K, cm³/mol	$\Delta\rho/(\rho_P c_0)$, 1/mol
MNP/p-(EtCAc), fresh sample (36 h)	−28.39 ± 6.53	−(7.47 ± 1.72) × 10^{-2}	−26.45 ± 6.08	−(6.96 ± 1.60) × 10^{-2}
MNP/p-(EtCAc), old sample (10 days)	−2.13 ± 0.29	−(5.61 ± 0.76) × 10^{-3}	−1.95 ± 0.14	−(5.13 ± 0.37) × 10^{-3}

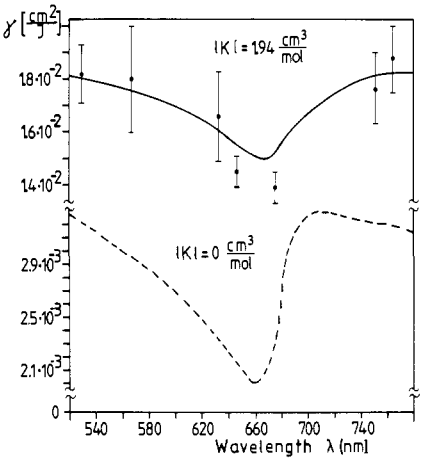

Figure 10. Normalized diffraction efficiency γ(λ) vs wavelength: calculated for pure photochemistry (---) and for photochemistry and an additional photomechanical effect (—). (●) Experimentally (PIH) measured values in a 10-day-old sample of MNP/p-(EtCAc).

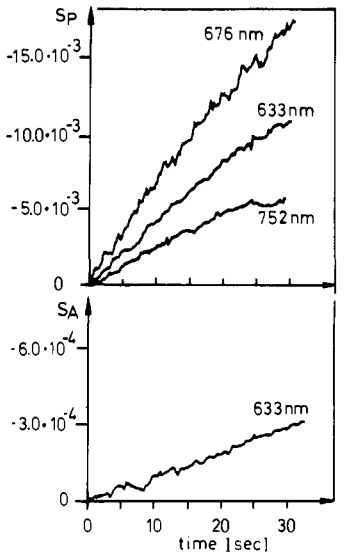

Figure 11. Signals proportional to the phase (P) and amplitude (A) contribution to the holographic grating monitored simultaneously for a 10-day-old sample of MNP/p-(EtCAc). $S_P = \sigma P$ and $S_A = \sigma A$ with the photodiode sensitivity σ(633 nm) = 0.40 A/W, σ(676 nm) = 0.45 A/W, and σ(752 nm) = 0.52 A/W.

reaction $\epsilon_{det}(\lambda)$ can be taken and $\Delta R_{PC}(\lambda)$ due to the photochemical transformation can be calculated with the help of eq 7. The resulting modulation amplitude of the refractive index $n_1^{PC}(\lambda)$, which is proportional to $\Delta R_{PC}(\lambda)$ (see eq 2a and 2b) is depicted in Figure 9 (dashed line). Accordingly, the wavelength dependence of the normalized diffraction efficiency γ(λ) can be calculated by taking $\Delta R_{eff} = \Delta R_{PC}$; i.e., $K = 0$ (see eq 6 and 8a). The graph γ(λ) is shown in Figure 10 (dashed line). On the other hand, γ(λ) was measured with PIH (see points in Figure 10). Note that the values of the holographic results are much higher than the values calculated from absorption spectra and that the shapes of the two graphs are different. The differences in the theoretical and experimentally measured values, γ(λ), correspond to differences between the change of molar refraction, responsible for hologram formation $\Delta R_{eff}(\lambda)$ and $\Delta R_{PC}(\lambda)$ (see section 2.1 and eq 8a). A change of the overall density is induced by the phototransformation of the RNO, leading to $K \neq 0$ in eq 8a and 8b.

For calculating the sign and value of K and the corresponding relative density change $\Delta\rho/(\rho_P c_0)$, P and A were measured directly with PMH (see eq 14a,b). From the ratio P/A, ΔR_{eff} was determined according to eq 9 and finally compared with ΔR_{PC} to yield K and $\Delta\rho/(\rho_P c_0)$ (see eq 8a,b).

In Figure 11 signals S_P, proportional to $P(t)$ measured for MNP in p-(Et-CAc) at 632.8, 676.4, and 752.5 nm, and S_A, proportional to $A(t)$ measured at 632.8 nm, are shown. Both $A(t)$ and $P(t)$ are negative over the whole range of wavelengths within the long-wavelength absorption band, resulting in a negative ΔR according to eq 9. In Table II ΔR_{PC}, P/A, ΔR_{eff} determined from PMH measurements, $|\Delta R_{eff}|$ determined from PIH measurements, and the corresponding K values for all three RNO in p-(EtCAc) and p-(MeCAc) measured at λ = 632.8 nm are compared. It can be seen from Table II that (i) ΔR_{eff} values determined by PMH and $|\Delta R_{eff}|$ values determined by PIH are in good agreement, (ii) K, i.e., the photomechanical contribution in eq 8a, dominates the photochemically induced change of molar refraction ΔR_{PC} by far, and (iii) K, i.e., $\Delta\rho/(\rho_P c_0)$, is negative (see eq 8a,b). Furthermore, the K values, within the limits of accuracy, do not depend on the specific phototransformed RNO but only on the matrix. K was found to be more than a factor of 2 smaller in fresh samples of p-(MeCAc) than in p-(EtCAc) (see Table II).

In Table III K values and the corresponding $\Delta\rho/(\rho_P c_0)$ values measured at two different wavelengths for samples of MNP in p-(EtCAc) of different ages are compared. Maximum achievable density changes are of a few percent for concentrations of RNO in the polymer between 0.3 and 0.8 mol/L and are comparable to density changes found for cis–trans photoisomerizations in cross-linked polymer networks.[31] K and $\Delta\rho/(\rho_P c_0)$ depend strongly on the age of the sample but not on the wavelength, as expected for K. Similar aging effects on K and $\Delta\rho/(\rho_P c_0)$ were found for TENC and NCPA in the polymer matrices.

With $K \neq 0$ and independent of wavelength the γ(λ) curves could be fitted according to eq 8a and 6, giving good agreement with the measured values (see Figure 10, full line). Note that the fitted curve closely resembles a transmission line shape of the near-IR *absorption* band, while a *dispersive* line shape should be expected for a hologram formation mechanism that is dominated by the phase grating contribution arising from the photochemical

Table IV. Holographic Sensitivity S (cm^2/J) for the Photopolymer Systems RNO/p-(Alkyl-CAc) Measured at Three Different Near-IR Wavelengths

λ, nm	MNP/p-EtCAc	MNP/p-MeCAc	TENC/p-EtCAc	TENC/p-MeCAC	NCPA/p-EtCAc	NCPA/p-MeCAc
			A. For Freshly Prepared Samples			
752	$(4.30 \pm 0.98) \times 10^{-3}$	$(8.37 \pm 1.50) \times 10^{-4}$	$(2.61 \pm 0.40) \times 10^{-2}$	$(4.95 \pm 0.69) \times 10^{-3}$	$(1.45 \pm 0.25) \times 10^{-4}$	$(2.57 \pm 0.61) \times 10^{-5}$
788	$(6.07 \pm 1.21) \times 10^{-5}$		$(1.28 \pm 0.30) \times 10^{-4}$			
799	$(1.86 \pm 0.69) \times 10^{-5}$		$(3.00 \pm 1.10) \times 10^{-5}$			
			B. For an Old Sample (10 days)			
752	$(3.45 \pm 0.79) \times 10^{-4}$	$(1.03 \pm 0.18) \times 10^{-4}$	$(2.53 \pm 0.39) \times 10^{-3}$	$(4.58 \pm 0.64) \times 10^{-4}$	$(1.20 \pm 0.17) \times 10^{-5}$	$(2.14 \pm 0.24) \times 10^{-6}$

reaction (as indicated by our measurements the contribution of the amplitude grating is negligible). This apparent discrepancy can be explained as follows: Since hologram formation over the whole range of wavelengths from 530 to 763 nm is caused mainly by a photomechanically induced pure phase grating, a large wavelength-independent contribution n_1^{MA} proportional to K adds to the small photochemically produced change of refractive index, $n_1^{PC}(\lambda)$ proportional to $\Delta R_{PC}(\lambda)$ (see Figure 9). Accordingly, the relative variation and the shape of $\gamma(\lambda)$ are determined by the wavelength dependence of the loss factor $D(\lambda)$ and *not* by the relatively small varying quantity $\Delta R_{eff}(\lambda)$.

We suggest that two possible mechanisms are responsible for the photomechanical effect in the photopolymer system RNO/p-(alkyl-CAc). First, alkyl and nitric oxide radicals generated in the primary photolytic step react with the polymer chains. The incorporation of NO or more probably of the larger alkyl radical may lead to a rearrangement of the polymer chains, thus producing the expansion of the polymer. Clearly, in p-(MeCAc) with its more rigid framework (i.e., higher T_g) expansion should be more limited than in p-(EtCAc).

Second, the reaction of the primary generated radicals with the polymer chains produces chain scission. Low molecular weight chain fragments usually correspond to a lower density.[34] In both mechanisms suggested the aging effect can be explained by different states of polymerization for fresh and old samples. Fresh polymer contains a considerably higher amount of low molecular weight components,[37,38] which can more easily rearrange and, on the other hand, produce smaller chain fragments (larger density changes) when scissioned.

Heating of the sample by absorption and successive radiationless relaxation seem to have neither influence on the photochemical nor on the hologram formation mechanism. We confirmed this by our measurements over a considerable intensity region ($I = 10^{-1}$ to $I = 10$ W/cm^2; see Figure 7) and by measurements with different beam radii (70 μm to 1 mm), i.e., different temperature gradients. The former yielded only the expected linear relation between the slope of the holographic growth curves $a^{1/2}$ and I due to photochemistry, and the latter showed that there is no influence of the beam radius on $a^{1/2}$.

4.3. Properties of the New Holographic Recording Material RNO/p-(Alkyl-CAc). Due to the unique combination that the RNO compounds absorb light in the near-IR wavelength region and have weak C–N bond dissociation energies,[13] they are the ideal photoreactive components in polymer systems, suitable for applications in the wavelength region of GaAlAs lasers. Indeed it was possible to record holograms in MNP/p-(EtCAc) and TENC/p-(EtCAc) with a GaAlAs laser at 788 nm (see Figure 12).

An important material parameter characterizing a photopolymer for holographic recording is its photosensitivity S, which can be defined by[39]

$$S = \eta^{1/2}/It \qquad (16)$$

S is obtained from linearized holographic growth curves as shown in Figure 12. The sensitivity values for the various systems

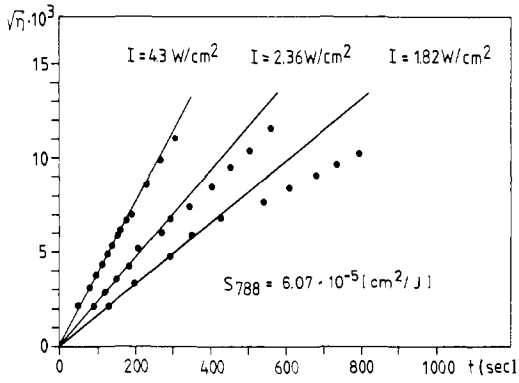

Figure 12. Linearized holographic growth curves recorded with a GaAlAs laser at λ = 788 nm in a fresh sample of MNP/p-EtCAc.

RNO/p-(alkyl-CAc) are compared in Table IV for three different near-IR wavelengths. For the geminal chloronitroso compound NCPA no sensitivity at 788 and 799 nm was measurable, because of the absorption maximum lying at a shorter wavelength (see Table I). The values of S in Table IVA were found for fresh samples of MNP, TENC, and NCPA in p-(alkyl-CAc) with identical concentrations of 0.3 mol/L and thicknesses of 460 μm. Differences in S at the same wavelength arise from differences in the quantum yield, ϕ, and the extinction coefficient of the RNO, ϵ_{rec}. With increasing age of the photopolymer samples the photosensitivity S decreases according to the decreasing value of the photomechanical parameter K (see Table IV). Diffraction efficiencies η of about 50% were achieved with a corresponding change of refractive index Δn of 1.26×10^{-3}. S, η, and Δn depend on the thickness of the sample and on the concentration of the RNO and can be considerably increased by increasing these parameters. S, η, and Δn were found to be independent of the fringe spacing Λ within the region Λ = 4.3–0.75 μm. Thus a resolution of at least 1.33×10^3 fringes/mm can be achieved in the RNO/p-(alkyl-CAc) systems.

From Table IV it can be seen that according to quantum yields and density changes the sensitivities for RNO dissolved in p-(MeCAc) are smaller than in p-(EtCAc) at λ = 752 nm.

The RNO photosensitivities *in the near-IR* are of the same order of magnitude as the photosensitivities of the best photopolymer systems known to date in the UV–visible region.[5] Still rather high recording intensities are needed, which can be supplied by commercial semiconductor lasers, however. Note that the relatively high sensitivities found in RNO/p-(alkyl-CAc) arise mainly from density changes generated in the polymer matrix. There might be perhaps other polymer hosts where an even larger photomechanical effect could be induced, but this point requires further investigation.

Compared to the photosensitivities of previously known near-IR-sensitive photopolymer systems, e.g., biacetyl dissolved in p-(EtCAc) ($S_{752} = 1.54 \times 10^{-5}$ cm^2/J)[7] and pure p-(EtCAc) containing residual monomer ($S_{752} = 2.7 \times 10^{-5}$ cm^2/J),[6] the photosensitivities of RNO/p-(alkyl-CAc) are 2–3 orders of magnitude larger.

Biacetyl/p-(EtCAc) and pure p-(EtCAc) are two-photon, four-level materials;[3,4,6,7] i.e., holographic recording occurs only by the subsequent absorption of one photon in the UV and one photon in the IR. (For the values of S mentioned a power density of 1 W/cm^2 was assumed for the first absorption step in the UV,

(37) Skeist, J. *Handbook of Adhesives*; Reinhold: New York, 1962; pp 409–414.
(38) Schering AG Berlin/Bergkamen, private communication.
(39) Bartolini, R. A.; Bloom, A.; Weakliem, H. A. *Appl. Opt.* **1976**, *15*, 1261–1266.

which is included in S.[6,7]) Reading is accomplished in these materials in the IR with the UV light source turned off; i.e., no photochemistry occurs during the reading process. Therefore no reduction of the recorded diffraction efficiency occurs; the hologram is self-developing. RNO in p-(alkyl-CAc) are one-photon, two-level materials, which need a development process to allow nondestructive reading. However, such a development is easily accomplished by sublimating the residual RNO from the polymer. This works excellently because of the high vapor pressure of the RNO.

Concerning the demand for nondestructive reading, two-photon materials are more advantageous compared to one-photon materials. But due to the fact that a two-photon process in general shows a smaller cross section than a one-photon process, both mechanisms should be kept in mind for developing new photopolymer systems with high photosensitivity in the near-IR. However, from our results the main question seems to be whether a considerable photomechanical effect can be induced in the polymer matrix. Only this enhancement effect may provide the high photosensitivity required for an efficient holographic recording material, as was demonstrated here with RNO/p-(alkyl-CAc).

5. Conclusion

A new class of near-IR-sensitive organic materials for holographic recording was found, consisting of tertiary nitrosoalkanes (RNO) as the photoreactive component and poly(alkyl α-cyanoacrylates) (p-(alkyl-CAc)) as the polymer matrix. After absorption of one photon at wavelengths up to 799 nm a homolytic dissociation of the C-N bond occurs in RNO, giving alkyl and nitric oxide radicals, which subsequently react with the polymer matrix. The last reaction step was found to be activation energy controlled. The quantum yield of the photoreaction of the RNO in the solid polymer matrix is relatively low compared to the quantum yield in liquid solution, probably because of the low mobility of the reaction partners and a high recombination rate of the primary produced radicals. Activation energies and quantum yields depend strongly on the glass transition temperature of the polymer, i.e., the rigidity of the framework of the polymer host.

The photochemical reaction of the RNO is accompanied by a considerable photomechanical effect leading to an expansion of the polymer matrix. Accordingly, a density decrease and thus a high change of refractive index are induced. Therefore, RNO in p-(alkyl-CAc) forms an excellent refractive index material with spectral sensitivity in the near-IR for various applications, e.g., integrated optics and holographic recording. The change of the refractive index due to the photomechanical effect is the dominant contribution to the overall change of refractive index and is found to depend strongly on the state of polymerization and composition of the polymer. The near-IR holographic sensitivities of the new materials were determined and were found to be about 3 orders of magnitude higher than the sensitivities of the two other known near-IR-sensitive organic holographic recording materials.[6,7] It was indeed possible to record holograms in RNO/p-(EtCAc) with a GaAlAs laser.

Acknowledgment. We are very grateful to the VW-Stiftung and the Fonds der Chemischen Industrie for support of this work. The helpful assistance of M. Piatkowski and the excellent electronic support of H. Horbach are gratefully acknowledged.

Chiral β-Cyclocitral Schiff Bases: A Combined Spectroscopic and Theoretical Approach to a Twisted Enimine Structure

Michael Klein, Ute Wingen, and Volker Buss*

Contribution from the Fachgebiet Theoretische Chemie der Universität Duisburg, D-4100 Duisburg, West Germany. *Received April 6, 1987*

Abstract: UV and CD spectra of eight β-cyclocitral Schiff bases rendered chiral by virtue of an asymmetrically substituted imine part have been measured and rationalized on the basis of force-field (MMP2) and quantum-mechanical (CNDO) calculations. They show the compounds to exist as a temperature- and solvent-dependent mixture of highly twisted s-cis and close to planar, but less stable s-trans conformers. Both $\pi\pi^*$ and $n\pi^*$ absorptions are unambiguously assigned, the former in the UV spectra and the latter in the CD spectra; however, only the sign of the $n\pi^*$ band correlates with the absolute conformation of the diene, being plus for M and minus for P helicity.

I. Introduction

Photochemically induced isomerization processes and conformational changes of protein-bound retinal play a central role in the primary reaction sequences that eventually result in a visual signal.[1] These changes involve mainly the open-chain chromophore of the protonated retinal Schiff base **1**; however, for detailed

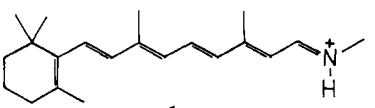

1

studies concerning, e.g., protein–chromophore interaction[2] or the peculiar spectral shifts observed for visual pigments,[3] the structure of the whole molecule, including the terminal β-ionone ring, has to be taken into account.

Because of severe steric interaction of the hydrogens on C7 and C8 with the methyl groups on C1 and C5, the preferred coplanar arrangement of the endocyclic double bond with the polyene chain is not possible. Instead, the molecule adopts a conformation derived from a twisted s-cis or s-trans arrangement along the C6–C7 linkage. In the solid state, *all-trans*- and 11-*cis*-retinal

(1) Kropf, A.; Hubbard, R. *Ann. N.Y. Acad. Sci.* **1958**, *74*, 266. Hubbard, R.; Kropf, A. *Proc. Natl. Acad. Sci. U.S.A.* **1958**, *44*, 130. Yoshizawa, T.; Wald, G. *Nature (London)* **1963**, *197*, 1279. Hurley, J.; Ebrey, G.; Honig, B.; Ottolenghi, M. *Nature (London)* **1977**, *270*, 540.

(2) Liu, R. S. H.; Mead, D.; Asato, A. E. *Proc. Natl. Acad. Sci. U.S.A.* **1985**, *82*, 259. Liu, R. S. H.; Mead, D.; Asato, A. E. *J. Am. Chem. Soc.* **1985**, *107*, 6609.

(3) Tabushi, I.; Shimokawak, K. *J. Am. Chem. Soc.* **1980**, *102*, 5402. Nakanishi, K.; Balogh-Nair, V.; Arnaboldi, M.; Tsujimoto, K.; Honig, B. *J. Am. Chem. Soc.* **1980**, *102*, 7945. Sheves, M.; Nakanishi, K. *J. Am. Chem. Soc.* **1983**, *105*, 4033. Baasov, T.; Sheves, M. *J. Am. Chem. Soc.* **1985**, *107*, 7524.

0002-7863/87/1509-6486$01.50/0